BIOCHEMISTRY
including biophysical chemistry & molecular biology

Article

pubs.acs.org/biochemistry

Sav1866 from *Staphylococcus aureus* and P-Glycoprotein: Similarities and Differences in ATPase Activity Assessed with Detergents as Allocrites

Andreas Beck,[†,§] Päivi Äänismaa,[†,∥] Xiaochun Li-Blatter,[†] Roger Dawson,[‡] Kaspar Locher,[‡] and Anna Seelig*[,†]

[†]Biozentrum, University of Basel, Division of Biophysical Chemistry, Klingelbergstrasse 50/70, CH-4056 Basel, Switzerland
[‡]ETH Zürich, Institute of Molecular Biology and Biophysics, HPK D17 Schafmattstrasse 20, CH-8093 Zürich, Switzerland

ABSTRACT: The ATP-binding cassette exporters Sav1866 from *Staphylococcus aureus* and P-glycoprotein are known to share a certain sequence similarity and disposition for cationic allocrites. Conversely, the two ATPases react very differently to neutral detergents that have previously been shown to be inhibitory allocrites for P-glycoprotein. To gain insight into the functional differences of the two proteins, we compared their basal and detergent-stimulated ATPase activity. P-Glycoprotein was investigated in NIH-MDR1-G185 plasma membrane vesicles and Sav1866 in lipid vesicles exhibiting a membrane packing density and a surface potential similar to those of the plasma membrane vesicles. Under basal conditions, Sav1866 revealed a lower catalytic efficiency and concomitantly a more pronounced sodium chloride and pH dependence than P-glycoprotein. As expected, the cationic allocrites (alkyltrimethylammonium chlorides) induced similar bell-shaped activity curves as a function of concentration for both exporters, suggesting stimulation upon binding of the first and inhibition upon binding of the second allocrite molecule. However, the neutral allocrites (*n*-alkyl-*β*-D-maltosides and *n*-ethylene glycol monododecyl ethers) reduced P-glycoprotein's ATPase activity at concentrations well below their critical micelle concentration (CMC) but strongly enhanced Sav1866's ATPase activity even at concentrations above their CMC. The lack of ATPase inhibition at high concentrations of neutral of detergents could be explained by their comparatively low binding affinity for the transmembrane domains of Sav1866, which seems to prevent binding of a second inhibitory molecule. The high ATPase activity in the presence of hydrophobic, long chain detergents moreover revealed that Sav1866, despite its lower basal catalytic efficiency, is a more efficient floppase for lipidlike amphiphiles than P-glycoprotein.

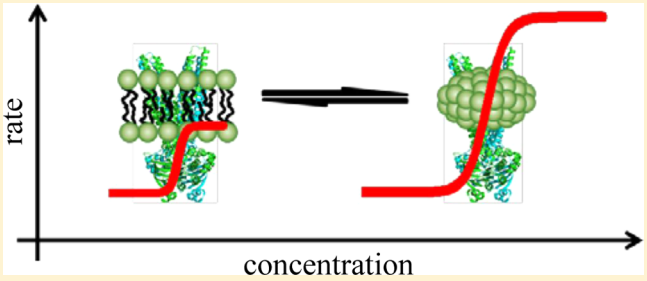

ATP-binding cassette (ABC) exporters, present in prokaryotes and eukaryotes, translocate or flop solutes (allocrites) from the cytoplasmic to the periplasmic leaflet of lipid bilayers (for a review, see ref 1). This mechanism serves different purposes. If allocrites are lipids as, e.g., in the case of the exporter MsbA from Gram-negative bacteria, it helps to preserve the lipid asymmetry of membranes (for a review, see ref 2); if allocrites are toxins or drugs as, e.g., in the case of the human P-glycoprotein (Pgp, ABCB1, and MDR1), it helps to protect the cytoplasm from intruding allocrites and is associated with multidrug resistance (for a review, see ref 3).

The minimal functional ABC exporter unit is formed by two cytoplasmic nucleotide-binding domains (NBDs) that bind and hydrolyze ATP to drive the transport cycle, and two transmembrane domains (TMDs), each comprising six *α*-helices that are responsible for allocrite recognition and translocation. Whereas the NBDs are highly conserved among ABC transporters, the TMDs are more diverse and generally determine allocrite specificity. Eukaryotic exporters such as Pgp consist of a polypeptide chain comprising all four domains and thus function as monomers, whereas prokaryotic exporters generally consist of a polypeptide chain comprising only one NBD and TMD and function as dimers. The putative exporter topography has originally been derived from hydropathy plots (for a review, see, e.g., ref 3).

In recent years, several structures from bacterial exporters of medium to high resolution became available, including that of the homodimer Sav1866 from the Gram-positive *Staphylococcus aureus* in the presence of ADP (determined at 3.0 Å resolution),[4] that of Sav1866 in the presence of the nonhydrolyzable ATP analogue AMP-PNP (determined at 3.4 Å resolution),[5] that of the homodimer MsbA from *Salmonella typhimurium* in the presence of AMP-PNP (determined at 3.7 Å resolution),[6] and that of the TM287–TM288 heterodimer from the thermophilic bacterium *Thermotoga maritima* (determined at 2.9 Å resolution).[7] Whereas the first three structures revealed an outward-facing state, the last one shows an inward-facing state. So far, the only eukaryotic exporter structure is that of Abcb1a (Mdr3) from

Received: June 19, 2012
Revised: April 19, 2013
Published: April 20, 2013

   dx.doi.org/10.1021/bi400203d | *Biochemistry* 2013, 52, 3297–3309

Mus musculus, which is a close homologue of human Pgp. It was crystallized in the apo form, and the structure (determined at 3.8 Å resolution) revealed an inward-facing state with NBDs wide apart.[8] As first described for Sav1866,[4] the individual TMDs are not simply aligned with each other as independent helical bundles but rather embrace each other and have a significant twist. The at first unexpected interface between TMD2 and NBD1 in Sav1866 was confirmed for Pgp using the reactivity of the sulfhydryl side chains of cysteines.[9] Despite related structural features of Pgp (Mdr3) and Sav1866, sequence identity and similarity vary markedly across the proteins; the sequences of NBD1 and NBD2 are 48 and 44% identical and 80 and 78% similar, respectively, whereas TMD1 and TMD2 show only a low level of sequence identity (<20% in both) and sequence similarity (56 and 52.8%, respectively).[10]

This structural information supports the alternating access model,[11] in which ABC transporters cycle between an inward-facing allocrite-binding conformation and an outward-facing allocrite-releasing conformation, whereby each transition from an inward-facing to an outward-facing conformation corresponds to a translocation and release step. In this model, ATPase activity directly correlates with the effective rate of allocrite translocation, even though this is not always evident from measurements of apparent transport (e.g., bidirectional transport assays) because especially in the case of Pgp many allocrites can also cross the membrane by passive diffusion.[12,13]

The aim of this investigation was to gain insight into the similarities and differences in the function of the multidrug resistance exporters Pgp and Sav1866. The physiological function of Sav1866 is so far unknown; however, a previous functional analysis showed that cationic, hydrophobic compounds, known to be allocrites for Pgp, stimulated the ATPase activity of Sav1866 and were moreover transported by Sav1866.[14] During purification and reconstitution into model membranes, we observed that the two exporters reacted very differently with respect to electrically neutral detergents. In the course of these manipulations, the original bilayer membrane surrounding the protein is partially removed by detergent solubilization, which leaves the exporter surrounded by mixed detergent/lipid micelles.

We previously showed that the ATPase activity of Pgp[15−17] was stimulated by cationic and certain electrically neutral detergents in a concentration-dependent manner, yielding bell-shaped activity curves that are best interpreted with a kinetic two-site binding model.[18,19] The model assumes activation upon binding of the first and inhibition upon binding of the second allocrite molecule. We further showed that ATPase activation by electrically neutral detergents occurred only if the affinity of the detergent's hydrophobic alkyl chain for the lipid membrane, ΔG^0_{lw}, and the affinity of the detergent's hydrogen bonding headgroup for the exporter, ΔG^0_{tl}, exhibited a specific, balanced ratio ($q \approx 2.7$).[16] Higher q values as determined, e.g., for the very hydrophobic detergent *n*-dodecyl β-D-maltoside (C_{12}-malt)[17,20,21] significantly reduced the ATPase activity and the concomitant rate of allocrite flopping by Pgp even at concentrations well below the critical micelle concentration (CMC). On the basis of deuterium nuclear magnetic resonance measurements, membrane disordering as a cause of Pgp inhibition by these detergents could be fully excluded.[17] Conversely, the ATPase activity of Sav1866 was highly activated by diverse detergents, including $C_{12}EO_8$ and C_{12}-malt.[4]

To answer the intriguing question of why Sav1866 and Pgp reacted so differently to electrically neutral detergents, we reconstituted Sav1866 in lipid vesicles formed from *Escherichia coli* polar lipid extract and egg yolk phosphatidylcholine [3:1 (w/w)] and compared it with Pgp in mouse embryo fibroblasts (NIH-MDR1-G185). First, we investigated the kinetics of ATPases in their basal state as a function of ATP concentration, sodium chloride concentration, and pH and determined the concentration of vanadate required to trap the exporters in the posthydrolysis state.[22] Second, we investigated the transition from lipid vesicles to detergent/lipid micelles. For this purpose, we titrated the ATPases with different detergents over a broad range up to concentrations above the CMC. As nonionic detergents, we investigated $C_{12}EO_8$ and C_{12}-malt that were used for purification and reconstitution,[4] as well as *n*-tetradecyl β-D-maltopyranoside (C_{14}-malt). With this choice of detergents, we obtained two pairs of allocrites, one exhibiting the same chain length and different headgroups and one exhibiting the same headgroup and different chain lengths. For comparison, we also used the cationic detergents dodecyltrimethylammonium chloride (C_{12}-TAC) and tetradecyl trimethylammonium chloride (C_{14}-TAC). Third, we assessed the allocrites' partition coefficients for the lipid membrane, K_{lw}, and the allocrites' binding constants for the exporters, K_{tw}.[16,19]

The analysis revealed that Sav1866 exhibits a lower basal catalytic efficiency in lipid vesicles and is more sensitive to variations in sodium chloride concentration and pH than Pgp. Most importantly, it revealed that Sav1866 was activated by cationic detergents in a manner similar to that of Pgp but was also activated by very hydrophobic electrically neutral detergents that inhibited Pgp. This suggests that Sav1866 is a more efficient floppase of hydrophobic amphiphiles than Pgp.

MATERIALS AND METHODS

Compounds. Octaethylene glycol monododecyl ether ($C_{12}EO_8$ or $C_{12}E_8$) was obtained from Fluka (Buchs, Switzerland). *n*-Nonyl β-D-maltoside (C_9-malt), *n*-decyl β-D-maltoside (C_{10}-malt), *n*-dodecyl β-D-maltoside (C_{12}-malt), *n*-tetradecyl β-D-maltoside (C_{14}-malt), dodecyltrimethylammonium chloride (C_{12}-TAC), and tetradecyltrimethylammonium chloride (C_{14}-TAC) were from Affymetrix (Cleveland, OH). 3-[(3-Cholamidopropyl)dimethylammonio]-1-propanesulfonate (CHAPS) was from Sigma. Bicinchoninic acid (BCA) assay reagents were purchased from Pierce (Rockford, IL). Bovine serum album (BSA) was from Sigma, and egg yolk phosphatidylcholine (POPC) and *E. coli* polar lipid extract were from Avanti Polar Lipids (Alabaster, AL). All other chemicals were obtained from Sigma or Merck.

Buffers. Experiments were performed in HEPES or Tris-HCl buffer (25 mM) containing 10 mM $MgSO_4$ and 150 mM NaCl adjusted to pH 7.5 at 25 °C unless otherwise mentioned. ATP was added in buffered solution to the reaction mixture to a final concentration of 7 mM, unless otherwise mentioned. Experiments with Pgp in inside-out plasma membrane vesicles from MDR1 transfected mouse embryo fibroblasts (NIH-MDR1-G185) were performed in the same buffer (including in addition 0.5 mM EGTA, 2 mM ouabain, and 3 mM sodium azide). It was adjusted to pH 7.4 at 25 and 37 °C. The pH dependence of the exporter's ATPase activity was measured in the pH range of 5.0−9.0 using different buffers (25 mM) containing 150 mM NaCl, 7 mM ATP, and 10 mM $MgSO_4$ at 25 °C: MES (25 mM at pH 5.0−6.4), HEPES (25 mM at pH 6.8−8.4), and Tris-HCl (25 mM at pH 8.5−9.0).

Purification and Reconstitution of Sav1866 into Lipid Vesicles and Detergent Micelles. Purification was described in detail elsewhere.[4] Briefly, the gene encoding Sav1866 fused to an N-terminal His tag was overexpressed in *E. coli*, solubilized, and purified in $C_{12}EO_8$. Sav1866 was reconstituted in lipid vesicles according to the protocol described for BtuCD.[23] The lipid vesicles used for reconstitution were composed of egg yolk PC and *E. coli* polar lipid extract [1:3 (w/w)] (see ref 4 for details). *E. coli* polar lipid extract contains phosphatidylethanolamine, phosphatidylglycerol, and cardiolipin [67:23.2:9.8 (w/w)]. Mixed lipid/$C_{12}EO_8$ micelles containing Sav1866 were formed by adding $C_{12}EO_8$ at a concentration ($C_{C_{12}EO_8}$) of 1.8 mM, which is ~20-fold the CMC (for CMCs, see Table 2).

In the course of the removal of the detergent by Bio-Beads SM2, the lipid and protein concentrations decreased and were therefore determined in the final proteoliposomes. The lipid concentration was quantified by a colorimetric phosphate assay[24] and the protein concentration by means of the BCA assay using a BSA standard. The lipid concentration was determined to be 4 mg/mL, i.e., 4400 μM, and the protein concentration was determined to be 1.84 ± 0.2 mg/mL, i.e., 14.2 μM (in 2.2 mM $C_{12}EO_8$). For comparison, the protein concentration was also determined by the method of Edelhoch.[25] For this purpose, the lipid vesicles were solubilized in a $C_{12}EO_8$ solution (2.2 mM) and equilibrated for 30 min. The solution was then diluted, and guanidinium chloride was added to a final concentration of 6 M. The molar extinction coefficient, *E*, was measured at 280 nm, and the corresponding protein concentration was calculated according to the method of ref 26 (http://www.expasy.ch/tools/protparam-doc.html), yielding 1.97 mg/mL or 15.2 μM, in close agreement with the data from the BCA assay (see above). The lipid:protein ratio was determined to be 312:1.

ATPase Assay. Sav1866-associated ATP hydrolysis was assessed in a 96-well microtiter plate (Nunc F96 MicroWell plate, nontreated) according to the method of Litman et al.[18] with small modifications.[27] The amount of ATP hydrolyzed increased linearly with concentration in the concentration range of 0.2−1.2 μg of Sav1866 per 60 μL of reaction mixture (C_{Sav} = 0.028−0.154 μM), yielding a constant ATPase activity. Experiments were performed with ~0.9 μg of protein/60 μL (C_{Sav} = 0.114 μM), except experiments shown in Figure 3, which were conducted with ~0.2 μg (C_{Sav} = 0.028 μM).

Sav1866 in lipid vesicles showed a linear activity increase up to 40 min at 25 and 37 °C. With mixed lipid/$C_{12}EO_8$ micelles, the activity increased linearly up to 40 min at 25 °C and up to only ~10 min at 37 °C. The level of exposure of NBDs to the outside of the plasma membrane vesicle was 80% (see Results).

The average protein content in plasma membranes of NIH-MDR1-G185 cells was 99 ± 1.7 mg/mL, and Pgp amounted to 1.1 ± 0.3% of the total protein concentration. The exposure of NBDs to the outside of the plasma membrane vesicle was close to 100%. The incubation time for phosphate release was 1 h at 25 and 37 °C (for details, see ref 27). To correct for nonspecific ATP hydrolysis induced by the acidic color reagent, the optical density (OD) of a sample containing proteoliposomes kept on ice during incubation was subtracted from the optical density of the sample. The optical density (OD) of the background control was ~0.04−0.2 and that of the sample 0.1−0.7, depending on the temperature and pH. The ATPase activity was inhibited with sodium orthovanadate (vanadate), which was depolymerized and thus activated prior to use by being boiled under basic conditions (pH 10).[28]

Cell Lines and Cell Culture. Mouse embryo fibroblast cell lines NIH3T3 and NIH-MDR1-G185 (grown in the presence of colchicine) were generous gifts from M. M. Gottesman and S. V. Ambudkar (National Institutes of Health, Bethesda, MD). The cells were maintained as described previously.[29,30]

Isothermal Titration Calorimetry (ITC). ITC demicellization experiments were performed with a VP-ITC calorimeter from MicroCal (Northampton, MA) to assess the CMC under the buffer conditions used for the ATPase activity assays. Briefly, the syringe was filled with a micellar detergent concentration usually 10-fold higher than the CMC. The calorimeter cell was filled with matching buffer [e.g., 25 mM HEPES, 150 mM NaCl, and 10 mM $MgSO_4$ (pH 7.5) at 25 °C]. All solutions were degassed before filling. The temperature was kept constant at 25 °C. A concentrated detergent solution for which $C \gg$ CMC was injected in small steps into buffer, and the heat of demicellization, δh_i, was recorded. Typically, 29 injections (10 μL each) were sufficient to go from complete disintegration of micelles (demicellization) to the situation where micelles no longer disintegrated.[31] The binding of $C_{12}E_8$ to lipid vesicles was performed using an ITC-200 instrument from Microcal. The cell volume was 203.7 μL and the injection volume 2 μL.

Light scattering and surface potential measurements were performed with a Zetasizer Nano-ZS instrument (ZEN3600; Malvern Instruments, Worcestershire, U.K.) as described previously.[31]

Circular Dichroism (CD) Measurements. CD spectra of Sav1866 (C_{prot} = 0.8 μM) reconstituted in lipid vesicles (C_{lip} = 163.9 μM) were measured in the presence of detergents at concentrations above the CMC [$C_{12}EO_8$ (1.8 mM), C_{12}-malt (1.8 mM), and C_{14}-TAC (2 mM)] in ATPase assay buffer [25 mM HEPES, 150 mM NaCl, and 10 mM $MgSO_4$ (pH 7.5) at 25 °C]. The buffer was filtered through a regenerated cellulose filter with a 0.2 μm pore size prior to use. Detergents were mixed with proteoliposomes 30 min before measurements to ensure complete solubilization. A blank sample contained *E. coli* polar lipid extract and POPC in a 1:3 (w/w) ratio and detergent at the same concentration as in proteoliposomes. The path length of the cuvette was 0.2 mm, and the bandwidth was adjusted to 2 nm. The percentage of protein secondary structure was estimated from a computer simulation based on a linear combination of α-helix, β-sheet, random coil, and β-turn reference spectra taken from ref 32.

Kinetic Data Analysis. Data were analyzed using the Michaelis−Menten equation

$$V_S = \frac{V_{max} C_S}{K_M + C_S} \quad (1)$$

where V_S denotes the reaction velocity, V_{max} the maximal reaction velocity, C_S the substrate (ATP) or allocrite concentration, and K_m the Michaelis−Menten constant. Alternatively, data were analyzed with the Hill equation

$$V_S = \frac{V_{max} C_S^{\,n}}{K_{0.5}^{\,n} + C_S^{\,n}} \quad (2)$$

where $K_{0.5}$ is the ATP or allocrite concentration at which the binding sites are 50% occupied and *n* the Hill coefficient. ATPase activity versus allocrite concentration curves were evaluated according to eq 3 if not otherwise mentioned[18,19]

dx.doi.org/10.1021/bi400203d | *Biochemistry* 2013, 52, 3297−3309

$$V_S = (K_1K_2V_0 + K_2V_1C_S + V_2C_S^2)/(K_1K_2 + K_2C_S + C_S^2) \quad (3)$$

where K_1 is the concentration of half-maximal activation, K_2 the concentration of half-maximal inhibition, V_0 the basal velocity, V_1 the activation velocity, V_2 the inhibition velocity, and C_S the aqueous allocrite concentration. The equations were fit to the data using a least-squares method.

Assessment of the Lateral Membrane Packing Density, π_M. The dominant parameters determining membrane partitioning are the lateral membrane packing density, π_M, and the surface potential, ψ, of the membrane on one hand and the cross-sectional area, A_D, and the charge, z, of the partitioning compound on the other.[19,33,34] As seen in eq 4, the membrane–water partition coefficient, K_{lw}, depends exponentially on these parameters

$$K_{lw} = K_0 e^{-\pi_M A_D/kT} e^{-zF\psi/RT} \quad (4)$$

where K_0 denotes a proportionality constant that is well represented by the air–water partition coefficient, K_{aw}, of the compound; kT the thermal energy per molecule; RT the thermal energy per mole; z the charge of the compound; and F the Faraday constant. The lateral packing density π_M can be assessed only indirectly, e.g., by comparing the lipid–water partition coefficients of a given compound for the bilayer with unknown lateral packing density (but known surface potential) with the partition coefficient of the same compound for a monolayer[35] or a bilayer[19] with known lateral packing density (and known surface potential) (see eq 4).

RESULTS

ATPase Activity of Sav1866 and Pgp as a Function of the ATP Concentration in the Absence and Presence of Sodium Chloride. The ATPase activity of Sav1866 in lipid vesicles (Figure 1A) and mixed lipid/$C_{12}EO_8$ micelles was measured as a function of ATP concentration using the phosphate release assay. The assay buffer [25 mM HEPES and 10 mM $MgSO_4$] without and with sodium chloride (C_{NaCl} = 150 mM) was adjusted to pH 7.5 at 25 °C. Further measurements were performed in the same buffer with sodium chloride at pH 7.0 and 37 °C. The activity increased with an increasing ATP concentration up to a maximum around 5–7 mM ATP and decreased again between 7 and 10 mM ATP (not shown) under all four buffer conditions. The decrease was more pronounced for conditions inducing higher ATPase activity (i.e., in the presence of $C_{12}EO_8$) and could be attributed to inhibition by ADP (i.e., product inhibition) (see also ref 36). Comparison of all four titration curves in Figure 1A shows that the ATPase activity increased in the following order: Sav1866 in vesicles with NaCl < Sav1866 in vesicles without NaCl < Sav1866 in mixed micelles with NaCl < Sav1866 in mixed micelles without NaCl (discussed in more detail below).

The ATPase activity of Pgp in inside-out vesicles formed from plasma membranes of NIH-MDR1-G185 cells (Figure 1B) was measured as a function of ATP concentration in an analogous buffer (see Materials and Methods) again without and with (C_{NaCl} = 150 mM) sodium chloride adjusted to pH 7.4 at 25 and 37 °C, respectively. In the case of Pgp, the maximal ATPase activity was reached at lower ATP concentrations and was less dependent on sodium chloride than in the case of Sav1866. Pgp in mixed lipid/$C_{12}EO_8$ micelles is not displayed in Figure 1B because it shows no activation as discussed below (see, e.g., Figure 4).

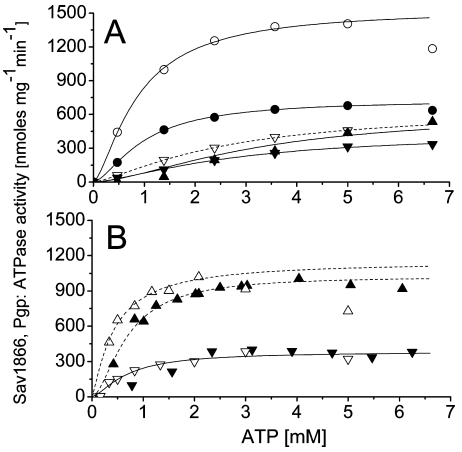

Figure 1. ATPase activity of Sav1866 and Pgp in lipid vesicle and mixed micelles as a function of ATP concentration in the absence and presence of sodium chloride. Basal ATPase activity in buffer (25 mM HEPES and 10 mM $MgSO_4$) with 150 mM NaCl (filled symbols) or without NaCl (empty symbols) measured as a function of ATP concentration. The buffer for Pgp further consisted of 0.5 mM EGTA, 2 mM ouabain, and 3 mM azide. (A) Sav1866 in lipid vesicles at pH 7.5 and 25 °C (▽ and ▼), in lipid vesicles at pH 7.0 and 37 °C (▲), and in mixed lipid/$C_{12}E_8$ micelles ($C_{12}E_8$; C = 1.8 mM) at pH 7.5 and 25 °C (○ and ●). (B) Pgp in NIH-MDR1-G185 plasma membrane vesicles at pH 7.4 and 25 °C (▽ and ▼) and at pH 7.4 and 37 °C (△ and ▲). The lines represent fits of the Hill equation (eq 2) to the data. Solid lines represent measurements at 25 °C and dotted lines those at 37 °C.

Titration curves were fit with the Michaelis–Menten (eq 1) and the Hill equation (eq 2), whereby better fits to the data were obtained with the latter equation. The solid lines in panels A and B of Figure 1 are fits to the Hill equation, and the corresponding kinetic constants are summarized in Table 1.

Whether the slightly sigmoidal shape of the titration curves (Hill coefficient $n > 1$) was indeed due to a low positive cooperativity for binding of ATP to the NBDs of the two exporters (see Table 1) or whether the apparent cooperativity was an artifact due to inhibition by ADP cannot be fully decided on the basis of the ATP release assay used for this analysis. Positive cooperativity of binding of ATP to NBDs was previously suggested for isolated NBDs of HlyB, another bacterial half-exporter,[37] and for MRP3.[38] In the case of HlyB, data were also obtained with a phosphate release assay. In the case of MRP3, data were obtained with a phosphate release assay and an ATP regeneration assay. Binding of ATP to Pgp measured with an ATP regeneration assay revealed no cooperativity.[39]

Figure 2 displays the influence of the extravesicular sodium chloride concentration on the ATPase activity of Sav1866 in lipid vesicles, whereby the intravesicular sodium chloride concentration remained constant. With a decreasing sodium chloride concentration, the basal rate of ATP hydrolysis by Sav1866 increased by a factor of >2, which is in good agreement with data shown in Figure 1A. Conversely, the ATPase activity of Pgp was barely dependent on the sodium chloride concentration as seen in Figure 1B.

Inhibition of the ATPase Activity of Sav1866 by Vanadate. Figure 3A shows inhibition of the ATPase activity of Sav1866 in lipid vesicles and mixed lipid/$C_{12}EO_8$ micelles by vanadate. Measurements were performed in buffer (25 mM HEPES, 7 mM ATP, and 10 mM $MgSO_4$) with varying sodium

dx.doi.org/10.1021/bi400203d | Biochemistry 2013, 52, 3297–3309

Table 1. Kinetic Constants of the Sav1866 ATPase Activity in the Absence and Presence of $C_{12}EO_8$

exporter	C_{NaCl} (mM)	T (°C)	pH	$K_{0.5}$ (eq 2) (mM)	n (eq 2)	V_{max} (eq 2) (nmol mg^{-1} min^{-1})	k_{cat} (eq 2) (s^{-1})	$k_{cat}/K_{0.5}$ (s^{-1} mM^{-1})[b]
Sav in vesicles	0	25	7.5	2.60 ± 0.17	1.35 ± 0.05	651 ± 26	1.4	0.54
Sav in vesicles	150	25	7.5	2.77 ± 0.39	1.47 ± 0.16	435 ± 38	0.9	0.34
Sav in vesicles	150	37	7.0	6.01 ± 3.44	1.70 ± 0.46	995 ± 486	2.2	0.36
Sav in micelles	0	25	7.5	0.88 ± 0.05	1.46 ± 0.11	1536 ± 46	3.3	3.78
Sav in micelles	150	25	7.5	0.99 ± 0.03	1.55 ± 0.06	730 ± 11	1.6	1.60
Pgp in vesicles	0	25	7.4	0.61 ± 0.08	1.63 ± 0.31	356 ± 20	1.0	1.65
Pgp in vesicles	0	27	7.4	0.65 ± 0.39	1.70 ± 1.24	675 ± 263	1.9	2.94
Pgp in vesicles	0	37	7.4	0.44 ± 0.09	1.20 ± 0.33	1153 ± 140	3.3	7.42
Pgp in vesicles	150	37	7.4	0.68 ± 0.04	1.70 ± 0.21	1025 ± 37	2.9	4.27

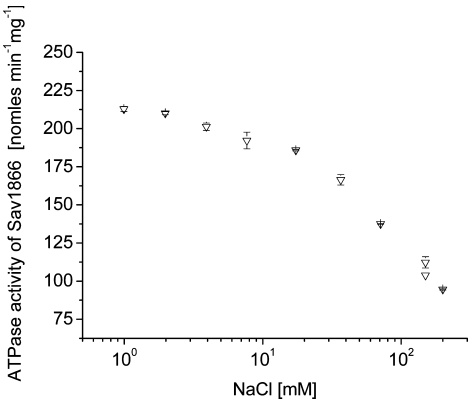

Figure 2. ATPase activity of Sav1866 in lipid vesicles measured as a function of sodium chloride concentration at pH 7.5 and 25 °C. The extravesicular sodium chloride concentration (C_{NaCl}) varied from 0 to 150 mM, while the intravesicular sodium chloride concentration remained constant (150 mM).

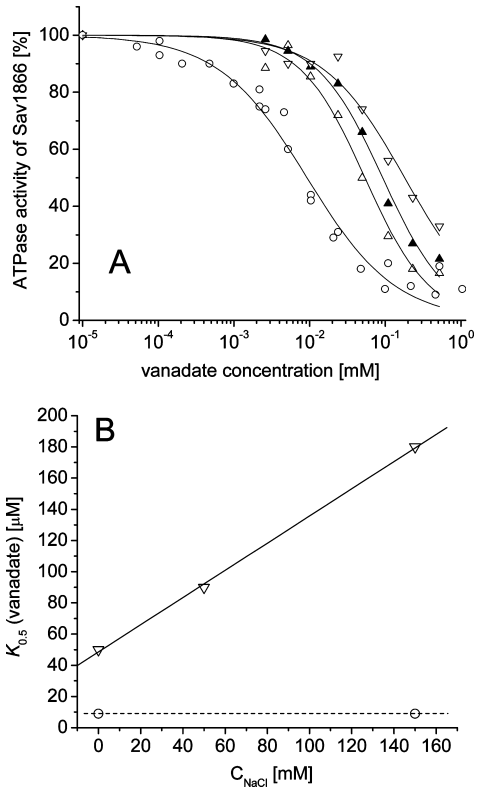

Figure 3. Inhibition of Sav1866's ATPase activity by vanadate. (A) ATPase activity of Sav1866 in lipid vesicles (triangles) and mixed lipid/$C_{12}E_8$ micelles (○) measured as a function of vanadate concentration at 25 °C and pH 7.5 with varying sodium chloride concentrations: 150 (▽), 50 (▲), and 0 mM NaCl (△). The solid lines are fits of the Hill equation (eq 2) to the data. (B) Concentration of half-maximal inhibition by vanadate plotted as a function of sodium chloride concentration. The solid and dotted lines are linear fits to the data.

chloride concentrations (C_{NaCl} = 0, 50, and 150 mM) adjusted to pH 7.5 at 25 °C. The concentrations of half-maximal inhibition by vanadate, $K_{0.5}$, were determined using the Hill equation (eq 2) and are displayed as a function of the sodium chloride concentration in Figure 3B. For Sav1866 embedded in lipid vesicles, the $K_{0.5}$ values increased linearly with sodium chloride concentration, whereas for Sav1866 embedded in mixed lipid/$C_{12}EO_8$ micelles, the $K_{0.5}$ values remained constant at a low level.

ATPase Activity of Sav1866 and Pgp as a Function of pH. The pH dependence of the ATPase activity of Sav1866 in lipid vesicles and mixed lipid/$C_{12}EO_8$ micelles was investigated in the range of pH 5.0–9.0 at 25 °C (Figure 4A). For this purpose, three different buffer systems, all containing 150 mM NaCl, were used (see Materials and Methods). The ATPase activity of Sav1866 in lipid vesicles showed a maximum at pH ~6.8 and decreased to negligibly low values below pH 5.0 and above pH 8.0. Data were fit to a Gaussian peak distribution yielding an optimum for ATP hydrolysis at pH 6.7 and half-maximal activity, $V_{50\%}$, at pH 5.9 and 7.6. In mixed micelles, the pH sensitivity decreased especially toward high pH values, yielding a somewhat asymmetric curve that could no longer be fit with a Gaussian peak distribution.

The pH dependence of Pgp in plasma membrane vesicles in the absence of allocrites was measured in an analogous manner at 32 °C (not shown) and 37 °C (Figure 4B). The pH dependencies of Pgp were similarly broad at both temperatures ($V_{50\%}$, at pH ~5.0 and ~9.0) and were broader than those of Sav1866 in lipid vesicles, especially toward high pH, which is in good agreement with previous measurements.[27,40] In mixed micelles [i.e., upon addition of the allocrite $C_{12}EO_8$ at a concentration ($C_{C_{12}EO_8}$) of 163.2 μM, which is above the CMC], the pH dependence of Pgp was similar in width and somewhat lower in activity over the whole pH range. Because $C_{12}EO_8$ induced maximal ATPase activity at low concentrations ($C_{C_{12}EO_8}$ = 1.6 μM) (see Figure 5A), we also measured the pH dependence of Pgp under these conditions. As seen in Figure 4B, the activity versus pH curve broadened further, again inducing higher activity toward high pH values.

ATPase Activity of Sav1866 in Lipid Vesicles upon Titration with Detergents. As shown above, the transition from a vesicular to a mixed micellar environment led to an ~2-fold increase in the ATPase activity of Sav1866 close to neutral

dx.doi.org/10.1021/bi400203d | Biochemistry 2013, 52, 3297–3309

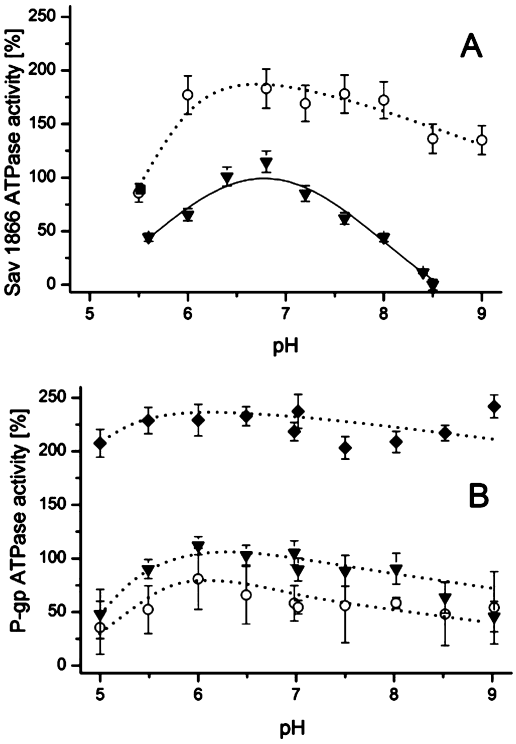

Figure 4. ATPase activity of Sav1866 and Pgp in lipid vesicles and mixed micelles plotted as a function of pH. Measurements were performed in the pH range of 5.0−9.0 using different buffers (25 mM) containing 150 mM NaCl, 7 mM ATP, and 10 mM $MgSO_4$, adjusted to the different pH values at 25 (A) and 37 °C (B). (A) ATPase activity of Sav1866 in lipid vesicles (▼) and mixed lipid/$C_{12}E_8$ micelles (○). (B) ATPase activity of Pgp in plasma membrane vesicles (▼), plasma membrane vesicles with $C_{12}E_8$ ($C_{C_{12}E_8}$ = 1.6 μM) (◆), and mixed lipid/$C_{12}E_8$ micelles ($C_{C_{12}E_8}$ = 163.2 μM) (○). For lipid vesicles, the average of five different measurements is shown, and for mixed lipid/$C_{12}E_8$ micelles, the average of two different measurements is shown. The activity vs pH curve for Sav1866 in lipid vesicles was fit with a Gaussian peak distribution (—). The activity vs pH curves for the other systems exhibiting higher catalytic efficiency were asymmetric (see the text), and the dotted lines were drawn to guide the eye.

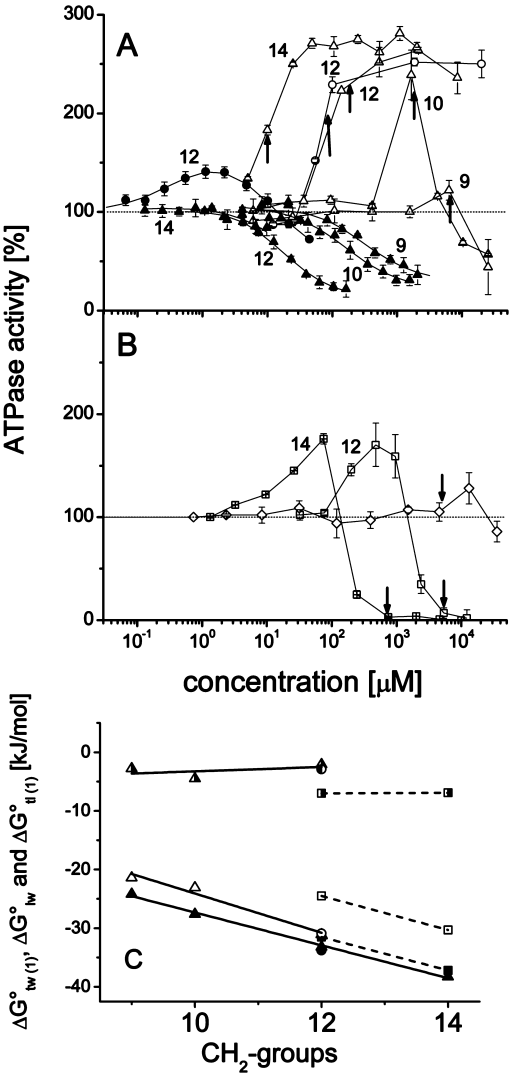

Figure 5. ATPase activity of Sav1866 as a function of detergent concentration. The Sav1866-ATPase in lipid vesicles was titrated with different detergents in buffer (25 mM HEPES, 150 mM NaCl, 7 mM ATP, and 10 mM $MgSO_4$) adjusted to pH 7.5 at 25 °C (empty symbols). For each detergent, the CMC is indicated by an arrow. The ATPase activity of Pgp measured in inside-out plasma membrane vesicles of mouse embryo fibroblasts (NIH-MDR1-G185) was included for comparison (filled symbols):[17] (A) C_{14}-malt (14, upward-pointing triangles), C_{12}-malt (12, upward-pointing triangles), C_{10}-malt (10, upward-pointing triangles), C_9-malt (9, upward-pointing triangles), and $C_{12}EO_8$ (12, circles) and (B) C_{14}-TAC (14, squares), C_{12}-TAC (12, squares), and CHAPS (diamonds). (C) Free energies of detergent binding from water to the exporter, ΔG^0_{tw} (empty symbols), free energies of partitioning of the detergent into the lipid membrane, ΔG^0_{lw} (filled symbols), and free energies of detergent binding from the membrane to the exporter, ΔG^0_{tl} (half-filled symbols). Values were calculated at 25 °C. Symbols for detergents as described above: maltosides (triangles), tetraethylammonium chlorides (squares), and $C_{12}EO_8$ (circles).

pH. To find the cause of this marked increase in activity, we studied the transition between the two environments by titrating Sav1866 in lipid vesicles with different detergents over a broad range of concentrations (~0.01 × CMC to 20 × CMC) under steady state conditions. Titrations were performed in buffer at 25 °C using nonionic ($C_{12}EO_8$, C_9-malt, C_{10}-malt, C_{12}-malt, and C_{14}-malt), cationic (C_{12}-TAC and C_{14}-TAC), and zwitterionic (CHAPS) detergents (Figure 5A,B). As seen in Figure 5A, the nonionic detergents activated Sav1866 below the CMC; thereby, the concentration of activity onset increased with a decreasing alkyl chain length. In the case of the longer and therefore less membrane disturbing[17] detergents (C_{14}-malt, C_{12}-malt, and $C_{12}EO_8$), the activity increased even above the CMC and remained at high levels over a broad concentration range. In the case of the shorter C_9-malt and C_{10}-malt, the activity decreased close to the CMC. The concentration of half-maximal activity, $K_{0.5}$, and the maximal rate, V_{max}, were estimated from the half-height and the maximal height of the curves, respectively, because the concentration of half-maximal activation was relatively close to the CMC and the activity increased slightly after the CMC, which may also partially be due to the exposure of intravesicular NBDs to the outside (see CHAPS below). The concentrations of half-maximal activity may therefore be slightly overestimated. The kinetic data are summarized in Table 2.

For the sake of comparison, data from previous, analogous titration experiments with the Pgp-ATPase[17] were included in Figure 5A. The solid lines are fits of eq 3 to the data. The

dx.doi.org/10.1021/bi400203d | Biochemistry 2013, 52, 3297−3309

concentrations of half-maximal activity, K_1, again increased with decreasing chain lengths; however, the values for half-maximal activity were more than 2 orders of magnitude lower for Pgp, and the maximal ATPase activity of Pgp was strongly reduced by C_{14}-malt, C_{12}-malt, and $C_{12}EO_8$ at higher concentrations relative to basal values. Thereby, it has to be noted that the long chain detergents reduced (or inhibited) the ATPase activity well below the CMCs in the case of Pgp (see Table 2), whereas they only activated it, even above the CMCs, in the case of Sav1866. The cationic detergents C_{12}-TAC and C_{14}-TAC (Figure 5B) enhanced the ATPase activity of Sav1866 at low concentrations and inhibited it at high concentrations. Analogous data for Pgp were not included because they virtually overlap with those of Sav1866 (for comparison, see ref 17).

Exposure of NBDs to the Extravesicular Side. The zwitterionic CHAPS neither activated nor inhibited the Sav1866-ATPase below the CMC, suggesting a lack of a direct interaction between CHAPS and Sav1866 (Figure 5B). The small increase in ATPase activity upon addition of CHAPS above the CMC could therefore be attributed to micellization of lipid vesicles and the concomitant exposure of luminal NBDs.[41] The increase in ATPase activity from a V_{max} of 80 nmol mg^{-1} min^{-1} in lipid vesicles (set to 100%) to a V_{max} of 101 nmol mg^{-1} min^{-1} in mixed micelles revealed that only 80% of the NBDs were oriented toward the extravesicular side in lipid vesicles, while 20% were occluded. This is in broad agreement with 93% of the NBDs oriented toward the extravesicular side in the case of BtuCD.[23]

Exporter–Water Binding Constant of Detergents. Binding of an allocrite to the lipid membrane and to the transmembrane domain of the exporter can be assumed to be much faster than allocrite transport. The concentration of half-maximal ATPase activation, $K_{0.5}$, can therefore be considered to be the dissociation constant of the allocrite for the aqueous phase, at least to a first approximation. The inverse can then be considered to be a binding constant of the allocrite from water to the transmembrane domain of the exporter, $K_{tw(1)}$. Because most allocrites for Sav1866 exhibit high lipid–water partition coefficients (Table 2), the allocrite concentration in the lipid phase is high and the allocrite concentration in the aqueous phase is low. Binding of an allocrite to Sav1866 is therefore likely to occur in two steps, a lipid–water partitioning step and an exporter–lipid binding step as described previously for Pgp.[19] The binding constant from water to the TMD of the exporter, $K_{tw(1)}$, can then be considered as the product of the lipid–water partition coefficient, K_{lw}, of the allocrite and the binding constant of the allocrite from the lipid membrane to the TMD, $K_{tl(1)}$, as described previously for other membrane-mediated ligand binding processes.[42,43]

$$1/K_1 \approx K_{tw(1)} = K_{lw}K_{tl(1)} \quad (5)$$

The detergent-induced concentrations of half-maximal activity, K_1, for Pgp and half-maximal binding, $K_{0.5}$, for Sav1866 differ by ~2 orders of magnitude (Figure 5A), although the lipid–water partition coefficients, K_{lw}, are practically identical for the two membranes (see the next paragraph).

Lipid–Water Partition Coefficients of Detergents. Partitioning of $C_{12}EO_8$ into lipid vesicles consisting of a mixture of *E. coli* polar lipid extract with egg yolk phosphatidylcholine [3:1 (w/w), concentration of 5.69 mM] was determined by ITC (Figure 6). For this purpose, a $C_{12}EO_8$ solution (62.4 μM) in buffer [10 mM Tris and 100 mM NaCl (pH 7.4)] was titrated with unilamellar lipid vesicles in the same buffer. Vesicles exhibited a diameter of 130 nm as assessed by dynamic light scattering. Injection of the lipid vesicles occurred in 2 μL steps at 25 °C. The lipid–water partition coefficient (K_{lw}) was determined to be 4425 ± 425 M^{-1}. Within error limits, the value is identical to the previously determined lipid–water partition coefficient of $C_{12}EO_8$ for POPC at 25 °C (K_{lw} = 4750 M^{-1}).[17] The lipid–water partition coefficients for the other detergents were therefore taken from previous investigations performed with POPC bilayers.[16,17] Data are summarized in Table 2.

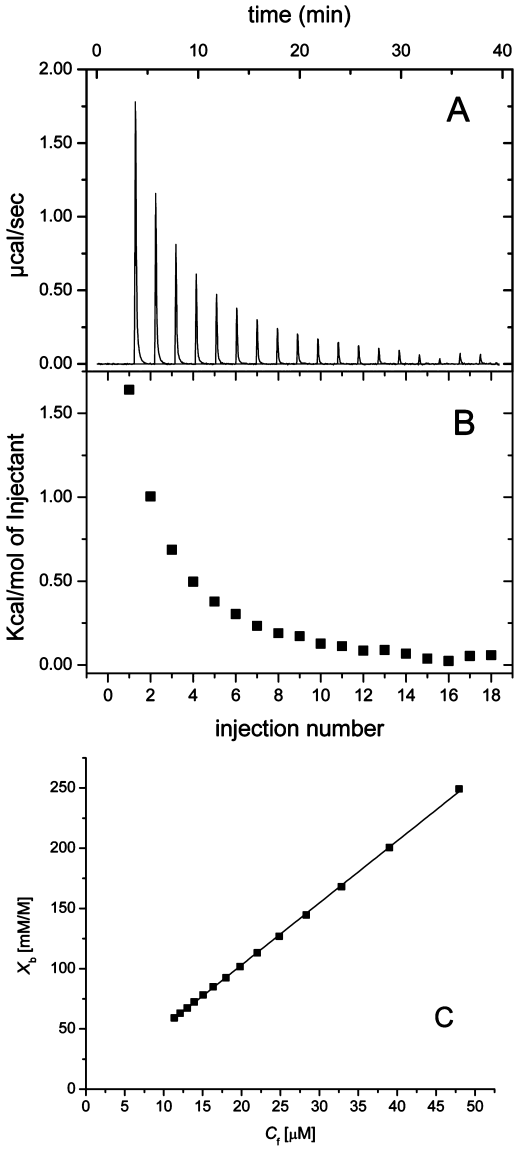

Figure 6. Measurement of $C_{12}E_8$ lipid–water partition coefficients by ITC. Titration of a 62.4 μM $C_{12}E_8$ solution in buffer [10 mM Tris and 100 mM NaCl (pH 7.4)] with unilamellar lipid vesicles in the same buffer. The diameter of the vesicles was ≈130 nm as determined by dynamic light scattering. Lipid vesicles consisted of *E. coli* polar lipid extract with egg yolk phosphatidylcholine [3:1 (w/w), concentration of 5.69 mM]. Injection of the lipid vesicles occurred in 2 μL steps at 25 °C. (A) Heat flow as a function of measurement time. (B) Heat per mole of injectant vs injection number. (C) Moles of detergent bound per mole of lipid (X_b) vs the free detergent concentration.

dx.doi.org/10.1021/bi400203d | *Biochemistry* 2013, 52, 3297–3309

Table 2. Thermodynamic and Kinetic Parameters

compound	K_{lw} (apparent) (M^{-1})	CMC (M)	$K_{0.5}$ [d] (M)	$\Delta G^0_{tw(1)}$ [c] (kJ/mol)	ΔG^0_{lw} (kJ/mol)	ΔG^0_{tl} (kJ/mol)	ΔG^0_{tl}(HA) (kJ/mol)
C_9-malt	100 [a]	6.54×10^{-3} [b]	3.14×10^{-3}	−24.2	−21.4	−2.8	−0.7
C_{10}-malt	200 [a]	1.82×10^{-3} [b]	8.09×10^{-4}	−27.6	−23.1	−4.5	−1.1
C_{12}-malt	5.0×10^3 [a]	1.87×10^{-4} [b]	8.52×10^{-5}	−33.2	−31.1	−2.1	−0.5
C_{14}-malt	not measured	1×10^{-5} [a]	1.07×10^{-5}	−38.3	not measured	not measured.	not measured
$C_{12}EO_8$	4.43×10^3 [b]	8.3×10^{-5} [b]	6.59×10^{-5}	−33.8	−30.8	−3.0	−0.4
C_{12}-TAC	350 [a]	5.25×10^{-3} [b]	1.68×10^{-4}	−31.5	−24.5	−7.0	−7.0
C_{14}-TAC	3.7×10^3 [a]	7×10^{-4} [a]	1.68×10^{-5}	−37.2	−30.3	−6.9	−6.9

[a]Taken from ref 17. [b]From this work: 25 mM HEPES, 150 mM NaCl, and 10 mM $MgSO_4$ (pH 7.5) at 25 °C. [c]Calculated at 25 °C according to the equation $\Delta G^0_{tw(1)} = -RT \ln C_w K_{tw(1)}$, where C_w = 55.5 mol/L. [d]$K_{0.5}$ corresponds to the concentration at $0.5V_{max}$.

The temperature dependence of the lipid−water partition coefficient, K_{lw}, is negligibly small for *n*-malts and *n*-glucs[44,45] as well as for *n*-TACs,[31] as seen from the very small enthalpies of binding, ΔH^0_{mem}. Partitioning of $C_{12}EO_8$ shows a somewhat higher temperature dependence, and the value of the lipid−water partition coefficient is therefore explicitly given ($K_{lw} = 6.5 \times 10^3$ M^{-1} at 37 °C). The free energy of lipid−water partitioning of $C_{12}EO_8$ (ΔG^0_{lw}) was then calculated as −30.8 kJ/mol at 25 °C and −32.9 kJ/mol at 37 °C according to eq 7 (see below).

Characterization of Lipid Vesicles Containing *E. coli* Polar Lipid Extract. As seen above, the lipid−water partition coefficient of $C_{12}EO_8$ was identical within error limits for POPC bilayers and bilayers formed from egg yolk PC and *E. coli* polar lipid extract [1:3 (w/w)]. The lateral packing density of POPC bilayers (π_M) was previously assessed as ∼32 mN/m at 25 °C.[35] Bilayers formed from egg yolk PC and *E. coli* polar lipid extract [1:3 (w/w)] at 25 °C can thus be assumed to exhibit a comparable lateral packing density. A decrease in lipid packing density of ∼2 mN/m is expected for an increase in temperature from 25 to 37 °C, which suggests a packing density (π_M) of ∼30 mN/m for bilayers of egg yolk PC and *E. coli* polar lipid extract [1:3 (w/w)] at 37 °C. This is in good agreement with the lateral packing density estimated for mouse embryo fibroblast plasma membranes (NIH-MDR1-G185) determined previously to be ∼30 mN/m at 37 °C.[19]

For the sake of comparison, we assessed the lateral packing density of vesicles consisting of POPC, instead of egg yolk PC, and *E. coli* polar lipid extract [1:3 (w/w)] as 34 mN/m at 25 °C based on a comparison of lipid−water partition coefficients of verapamil[46] (not shown). This value is close to the lateral packing density (35 mN/m) estimated previously for membranes consisting of pure *E. coli* polar lipid extract at ambient temperature.[47] The comparatively low packing density of mixtures containing egg yolk PC arises from packing density reducing components, e.g., lyso-lipids and fatty acids.

The ζ potential, which is the average electrostatic potential at the hydrodynamic plane, bears some relation to the surface potential.[48] It was measured for vesicles formed from egg yolk PC and *E. coli* polar lipid extract [1:3 (w/w)] as a function of magnesium sulfate concentration at 25 °C in buffer without sodium chloride. In the absence of magnesium chloride, the ζ potential was assessed as −43 mV. However, in the presence of 10 mM $MgSO_4$, it decreased to −3.7 mV. The ζ potential could not be measured in the presence of 150 mM NaCl used in most buffers but can be assumed to be even less negative. Under the conditions chosen, the negative surface potential for NIH-MDR1-G185 cells is negligible as well (see also ref 19).

Free Energy of Allocrite Binding from Water to the Exporter. The free energy of binding from water to the exporter (first binding site), $\Delta G^0_{tw(1)}$, can be expressed as the sum of the free energy of lipid−water partitioning, ΔG^0_{lw}, and the free energy of exporter−lipid binding (first binding site), $\Delta G^0_{tl(1)}$

$$\Delta G^0_{tw(1)} = \Delta G^0_{lw} + \Delta G^0_{tl(1)} \quad (6)$$

The free energy of lipid−water partitioning was determined as

$$\Delta G^0_{lw} = -RT \ln C_w K_{lw} \quad (7)$$

and the free energy of binding from water to the exporter as

$$\Delta G^0_{tw(1)} = -RT \ln C_w K_{tw(1)} \quad (8)$$

where C_w is the concentration of water (55.5 mol/L at 25 °C and 55.3 mol/L at 37 °C) and *RT* is thermal energy. The effective free energy of binding of the allocrite from the lipid membrane to the first binding region of the exporter, $\Delta G^0_{tl(1)}$, cannot be measured directly; however, it can be assessed as the difference between the free energy of exporter−water binding, $\Delta G^0_{tw(1)}$, and the free energy of lipid−water partitioning, ΔG^0_{lw} (see eq 6). The values of $\Delta G^0_{tw(1)}$, $\Delta G^0_{tl(1)}$, and ΔG^0_{lw} are displayed as a function of the hydrophobic anchor lengths of the detergents in Figure 5C. Linear regression analysis yielded an incremental free energy contribution per methylene group [$\Delta(\Delta G^0_{lw})_{CH_2}$] of approximately −3.3 kJ/mol, in good agreement with previously published data.[16,17] Because binding to

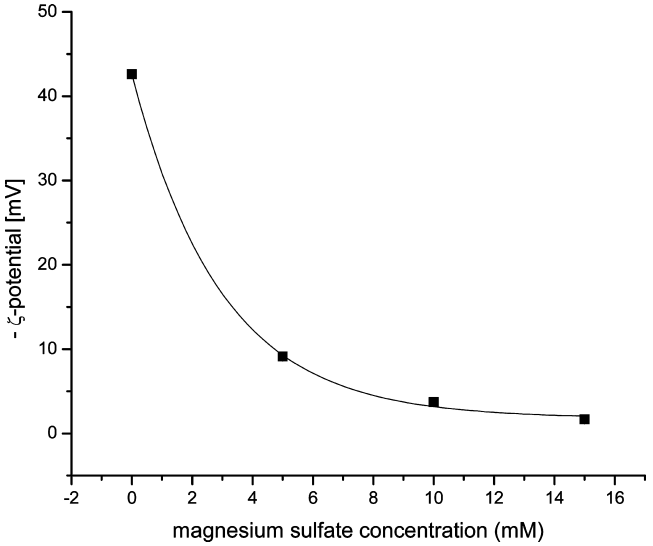

Figure 7. Measurement of ζ potentials. The ζ potential of vesicles formed from *E. coli* polar lipid extract and egg yolk phosphatidylcholine [3:1 (w/w)] was measured as a function of $MgSO_4$.

dx.doi.org/10.1021/bi400203d | *Biochemistry* 2013, 52, 3297−3309

Sav1866 is likely to occur in the lipid membrane, we assumed that the polar headgroups of the detergents bind to the exporter via hydrogen bond acceptor groups as demonstrated previously for Pgp. The free energy of binding, $\Delta G^0_{tl(1)}$, was divided by the number of hydrogen bond acceptor groups, yielding a free energy of binding per hydrogen bond acceptor group[15] $\{\Delta[\Delta G^0_{tl(1)}]_{HA}\}$ of -0.7 ± 0.3 kJ/mol. The affinity per quaternary ammonium ion in C_m-TAC $\{\Delta[\Delta G^0_{tl(1)}]_{HA}\}$ was assessed as -6.9 kJ/mol. This value is an upper limit calculated for an electrically neutral (or neutralized) membrane.[17]

Secondary Structure of Sav1866 Monitored by CD Spectroscopy at Detergent Concentrations above the CMC. To test the effect of detergents on the secondary structure of the exporter, we measured the CD spectra of Sav1866 in the presence of $C_{12}EO_8$, C_{12}-malt, and C_{14}-TAC at concentrations well above the CMC (Figure 8). In the presence of $C_{12}EO_8$ (C = 1.8 mM; CMC = 0.08 mM) and C_{12}-malt (C = 1.8 mM; CMC = 0.17 mM), the secondary structure of Sav1866 was assessed as ~66−68% α-helix, ~3−6% β-sheet, 16−24% random coil, and 4.5−11.5% β-turn and was thus comparable to that determined for the crystal structures (64% α-helix and 9% β-sheet[4] or 63% α-helix and 9% β-sheet),[5] which indicates the integrity of Sav1866 in mixed detergent/lipid micelles. In the presence of C_{14}-TAC (C_{TAC} = 2 mM; CMC = 0.7 mM), the secondary structure of Sav1866 exhibited a lower percentage of α-helix and a higher percentage of random coil conformation (~48% α-helix, ~21% β-sheet, 31% random coil, and 0% β-turn). In the case of TAC, the lack of activity at this high concentration may thus also be due to the decrease in the α-helicity of the TMDs.

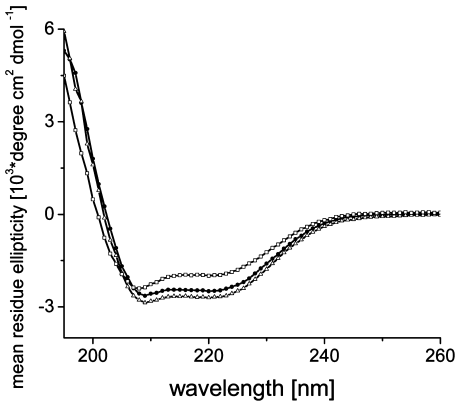

Figure 8. CD spectra of Sav1866 in mixed micelles. CD spectra of Sav1866 (C = 0.8 μM) in the presence of $C_{12}E_8$ (C = 1.8 mM) (●), C_{12}-malt (C = 1.8 mM) (△), and C_{14}-TAC (C = 2 mM) (□) in buffer [25 mM HEPES, 150 mM NaCl, and 10 mM $MgSO_4$ (pH 7.5)] at 25 °C. The concentration of lipids was 163.9 μM. Baseline measurements without Sav1866 were recorded and were subtracted.

DISCUSSION

The ATPase activity of Sav1866 in lipid vesicles and mixed lipid/detergent micelles was compared with the ATPase activity of Pgp in plasma membrane vesicles of NIH-MDR1-G185 cells and mixed lipid/detergent micelles. Although the two types of membranes differ in composition, detailed analysis revealed comparable packing densities and surface potentials, which warrants the following comparisons. Variation of ATP and sodium chloride concentrations, as well as the pH of the solution, revealed subtle differences in the function of the exporters' basal ATPase activity. Titration of the two exporters with cationic and electrically neutral detergents acting as allocrites showed similar kinetics for cationic detergents but surprisingly different kinetics for electrically neutral detergents. The differences can be traced back to different TMD−allocrite interactions as discussed in more detail below.

Sav1866 Exhibits a Lower Basal Catalytic Efficiency Than Pgp. The basal ATPase activity of the two exporters was measured as a function of ATP concentration at different temperatures and sodium chloride concentrations by means of the phosphate release assay (Figure 1), and data listed in Table 1 were obtained using the Hill equation (eq 2). The ATP concentrations yielding half-maximal ATPase activity, $K_{0.5}$, showed a weak dependence on temperature for both exporters as seen in Table 1. In lipid vesicles (in the absence of allocrites), the $K_{0.5}$ values were higher by a factor of 4−5 for Sav1866 than for Pgp. To give an example, the concentration of half-maximal activity for Sav1866 and Pgp in lipid vesicles at 25 °C ($K_{0.5}$) was assessed as ~2.6 and ~0.6 mM, respectively. The concentration of half-maximal activity for Sav1866 is in good agreement with the ATP dissociation constant determined previously for the lipid A floppase MsbA reconstituted into *E. coli* lipid membranes (K_d = 2.12 mM).[49] The concentration of half-maximal activity determined for Pgp is in broad agreement with the dissociation constant determined previously for Pgp reconstituted into lipid vesicles (K_d = 0.33 mM).[39]

In mixed lipid/$C_{12}EO_8$ micelles [i.e., the presence of allocrites (see below)], the half-maximal ATPase activity of Sav1866 decreased to ~0.9 mM. A decrease in the concentration of half-maximal activity, although less pronounced, was observed previously for Pgp in the presence of allocrites.[39]

In contrast to the concentrations of half-maximal activation, $K_{0.5}$, the maximal ATPase activity, V_{max}, was highly temperature dependent for both exporters, in good agreement with previous measurements of Pgp's temperature dependence.[50] The basal turnover numbers, k_{cat},[a] in lipid vesicles were similar under comparable conditions; however, the basal catalytic efficiency, $k_{cat}/K_{0.5}$,[b] was somewhat lower for Sav1866, because of the higher concentration of half-maximal activity ($K_{0.5}$).

Sodium Chloride Lowers the Rate of ATP Hydrolysis by Sav1866. The ATP concentrations yielding half-maximal ATPase activity, $K_{0.5}$, showed a weak dependence on the concentration of sodium chloride for both exporters as seen in Table 1. However, the maximal ATPase activity, V_{max}, showed a relatively high sodium chloride dependence for Sav1866 in lipid vesicles but not for Pgp in lipid vesicles (Figures 1A and 2).

Upon addition of hydrophobic long chain detergents acting as allocrites, the catalytic efficiency of Sav1866, $k_{cat}/K_{0.5}$, increased by a factor of 7 in the absence but by a factor of only 4.7 in the presence of sodium chloride (C_{NaCl} = 150 mM). The rate of ATP hydrolysis by Pgp (as well as the catalytic efficiency) decreased in the presence of long chain detergents (Figure 5A) as discussed in detail previously,[17] but the decrease was almost independent of the sodium chloride concentration.

Deceleration of ATP hydrolysis by increasing sodium chloride concentrations could have different molecular causes. As the sodium chloride concentration (e.g., in Figure 2) varied only in the extravesicular solution, while the intravesicular concentration remained constant, osmotic effects could a priori not be excluded.[51] Because the maximal ATPase activity of Sav1866, V_{max}, in mixed micelles, where osmosis plays no role, also increased by a factor of ~2 upon withdrawal of sodium

dx.doi.org/10.1021/bi400203d | *Biochemistry* 2013, 52, 3297−3309

```
                                  Walker A / Q-loop / Signature / Walker B / H-loop
Sav1866                 ----GMSGGGKST----Q----LSGGQ--ILILDEATSALD----H--
HlyB                    ----GRSGSGKST----Q----LSGGQ--ILIFDEATSALD----H--
ABCB1 (human) nt        ----GNSGCGKST----Q----LSGGQ--ILLLDEATSALD----H--
ABCB1 (human) ct        ----GSSGCGKST----Q----LSGGQ--ILLLDEATSALD----H–
Tap1                    ----GPNGSGKST----Q----LSGGQ--VLILDDATSALD----Q--
Tap1 (Q701H)            ----GPNGSGKST----Q----LSGGQ--VLILDDATSALD----H--
Tap1 (Q701H/D668E)      ----GPNGSGKST----Q----LSGGQ--VLILDEATSALD----H--
```

Figure 9. Sequence alignment of Sav1866 with other ABC exporters. The catalytically important amino acids in Walker B (glutamic acid) and the H-loop (histidine) are shown in bold.

Table 3. Different Conditions for ATPase Activity Assays Taken from the Literature[a]

protein	buffer	[buffer] (mM)	monovalent salt	[salt] (mM)	[$MgCl_2$] (mM)	[ATP] (mM)	pH	ref
Pgp	Tris	50	NH_4Cl	150	5	2	7.5	21
Pgp	Tris-HCl	25	KCl	50	2.5	3	7.0	18
Pgp	Tris-MES	50	*N*-methyl-D-glucamideCl	50	5	5–7.5	6.8	39
Sav1866	HEPES	25	NaCl	150	10	7	7.5	4
Pgp	Tris-H_2SO_4	50	–	–	15	10	7.4	55

[a]The different conditions are listed in order of increasing ATP concentration.

chloride (see Figure 1A), significant osmotic effects could be excluded. A strong sodium chloride dependence was also observed for the isolated NBDs of HlyB in solution.[37,52] The decelerating effect of sodium chloride seems thus to be due rather to direct electrostatic effects in the NBDs influencing ATP hydrolysis. In this context, it is interesting to note that the crystal structure of the nucleotide-bound Sav1866 generated in the presence of a relatively high sodium concentration (100 mM Na_2HPO_4) shows two sodium ions located close to Walker A,[4] which could indeed interfere with the function of the ATPase.

Sodium Chloride Enhances the Concentration of Half-Maximal Inhibition by Vanadate in Lipid Vesicles but Not in Micelles. For Sav1866 embedded in lipid vesicles (Figure 3B), the concentration of half-maximal inhibition by vanadate increased linearly with sodium chloride concentration from 50 μM (C_{NaCl} = 0 mM) to 180 μM (C_{NaCl} = 150 mM). The concentrations of half-maximal inhibition, $K_{0.5}$, for Sav1866 were thus higher than those determined previously for Pgp in multidrug-resistant Chinese hamster ovary cells (CR1R12) ($K_{0.5}$ = 9 μM, in the absence of NaCl)[22] and HlyB-NBDs in aqueous solution ($K_{0.5}$ = 16 μM).[52]

In the presence of allocrites (i.e., in mixed lipid/$C_{12}EO_8$ micelles), the concentration of half-maximal inhibition of Sav1866 by vanadate decreased significantly and reached a similar value ($K_{0.5}$ = 9 μM) as in the case of Pgp. Vanadate trapping in the posthydrolysis state of Sav1866 thus seems to be facilitated in the presence of allocrites, inducing a higher rate of ATP hydrolysis, as observed previously with activating allocrites for Pgp[39,53] and MRP3.[38] In the presence of allocrites, the concentration of half-maximal inhibition, $K_{0.5}$, of Sav1866 by vanadate remained constant, independent of the sodium chloride concentration. As ATP hydrolysis is coupled with proton release, an increase in the extent of ATP hydrolysis may lead to a slight local acidification that may, in turn, prevent sodium chloride accumulation and binding.

The pH Sensitivity of Exporters Decreased with an Increasing Catalytic Efficiency. Sav1866 ($V_{50\%}$ at pH ~5.9 and ~7.6) (Figure 4A) showed a narrow pH dependence compared to that of Pgp ($V_{50\%}$ at pH ~5.0 and ~9.0). At activating concentrations of the allocrite $C_{12}EO_8$, the pH sensitivity of Sav1866 and Pgp both decreased, especially at high pH values. Similarly narrow pH dependencies like that for Sav1866 have been observed previously for HlyB-NBDs in solution ($V_{50\%}$ at pH 6.1 and 8.2)[37] and the double mutant of TAP1-NBDs (D668E/Q701H) ($V_{50\%}$ at ~pH 5.0 and ~7.0), whereas a broader pH dependence has been reported for the single mutant of the TAP1-NBDs (Q701H)[54] (see Figure 9). Comparison of kinetic data for Sav1866 and Pgp on one hand and the three TAP-NBDs on the other suggests that within a given group a higher affinity for ATP (lower $K_{0.5}$) corresponds to a broader pH dependence (i.e., lower pH sensitivity) (see Table 1 for Sav1866/Pgp and ref 54 for TAP-NBDs).

The broadening of ATPase activity versus pH curves observed upon stimulation of ATP hydrolysis toward high pH values may be explained in the frame of the linchpin model.[37] The model is based on the crystal structure of HlyB-NBDs and suggests that histidine, H662, in its protonated form plays a key role in ATP hydrolysis. Stimulation of ATP hydrolysis leads to a higher rate of proton release and possibly to a concomitant decrease in the local pH value, which may in turn allow for histidine protonation, even at high bulk pH values.

Ideal Buffer Conditions for Measuring Sav1866's ATPase Activity. A broad range of buffers has so far been used in ATPase activity assays with ABC exporters. A few examples are summarized in Table 3 and show that the concentration of the monovalent salts and ATP varied strongly. These data show that the optimal basal ATPase activity of Sav1866 is obtained at intermediate ATP concentrations (C_{ATP} ~ 5 mM), low sodium chloride concentrations, and pH 6.8–7.4, i.e., under conditions that resemble those in the cytosol

quite closely. In contrast to basal values, the allocrite stimulated activity relative to basal values may even be higher close to pH 8.0. Measurement of the sodium chloride dependence provided interesting insight into the functional differences between Sav1866 and Pgp but has most likely no direct physiological significance. However, as demonstrated above, high ATP concentrations and correspondingly high magnesium chloride concentrations, high sodium chloride concentrations, and high pH lead to low basal rates of ATP hydrolysis, especially in the case of Sav1866, and may thus be favorable for exporter crystallization.

Cationic and Electrically Neutral Detergents Are Allocrites for Sav1866. As for Pgp,[16,17] binding of an allocrite to Sav1866 occurs in two steps, a lipid−water partitioning step and a binding step from the lipid membrane to the exporter. The former is driven by hydrophobic interactions, and the latter seems to be driven either by strong electrostatic interactions as in the case of the cationic C_m-TACs or (much more frequently) by hydrogen bond formation, i.e., weak electrostatic interactions, between hydrogen bond acceptors in the polar part of the electrically neutral detergents and hydrogen bond donors in the TMDs of the exporter. However, in the case of Sav1866, the free energy of binding per hydrogen bond acceptor in detergent allocrites was clearly less negative $\{\Delta[\Delta G^0_{tl(1)}]_{HA} \simeq -0.7$ kJ/mol$\}$ than in the case of Pgp $\{\Delta[\Delta G^0_{tl(1)}]_{HA} \simeq -1.8$ kJ/mol$\}$.[16,17]

According to Coulomb's law, electrostatic interactions become weaker with an increasing dielectric constant, ε, of the environment. The weaker hydrogen bonding (i.e., weak electrostatic) interactions of the detergents with the TMDs thus suggest a more polar environment in the binding region of Sav1866, which is consistent with the large polar cavity toward the cytosolic membrane−water interface observed in the crystal structure of Sav1866 (see Figure 4 of ref 4).

From a kinetic point of view, the greatest similarity between Sav1866 and Pgp was again observed for the cationic detergents C_{12}-TAC and C_{14}-TAC (Figure 5B) and is consistent with the ability of Sav1866 to transport cationic amphiphiles.[14] A striking difference in the kinetics of the two exporters was, however, observed for the uncharged detergents, $C_{12}EO_8$, C_{12}-malt, and C_{14}-malt (Figure 5A). Whereas all three detergents strongly enhanced the ATPase activity of Sav1866 up to concentrations above the CMC, $C_{12}EO_8$ enhanced the ATPase of Pgp only at low concentrations and reduced (or inhibited) it at higher concentrations, which were however still well below the CMC. C_{12}-malt inhibited Pgp at low concentrations. C_{14}-malt, the most hydrophobic detergent, inhibited the ATPase of Pgp, at even lower concentrations, however, only to a low extent, because the long hydrophobic anchor seems to be bound too tightly to the lipid environment to properly engage in the transport process.[17]

In the frame of the two-site binding model, where ATPase activation of Pgp occurs upon binding of a first molecule and inhibition upon binding of a second molecule to the translocation pathway of the exporter,[18] accommodation of the second molecule and thus inhibition seem possible only if the hydrogen bond affinity of the allocrite to the exporter is sufficiently high to overcompensate for the steric repulsive interactions that occur upon accommodation of a second molecule.[15,17,19] The lack of inhibition of Sav1866 by the hydrophobic detergents C_{12}-malt and C_{14}-malt suggests that the second inhibitory binding site is not occupied.

As shown previously,[15,17] C_{12}-malt induces a low rate of ATP hydrolysis by Pgp even if it is bound only to the first binding site, because of the unfavorable ratio between the affinity of the detergent's anchor for the lipid membrane and the affinity of the detergent's headgroup for the exporter ($q > 2.7$). Thereby, the former is reflected by the free energy of lipid−water partitioning, ΔG^0_{lw}, and the latter by the free energy of allocrite binding from the lipid membrane to the exporter, ΔG^0_{tl}. The strong activation by C_{12}-malt and C_{14}-malt shows that Sav1866 can handle compounds with a q ratio of >5 and thus has a significantly higher flopping power for hydrophobic compounds than Pgp.

CONCLUSIONS

The homodimeric Sav1866 exhibited a basal turnover number similar to that of Pgp under equivalent conditions, however, a higher concentration of half-maximal activation by ATP and thus a slightly lower catalytic efficiency (k_{cat}/K_d) than the monomeric Pgp. The basal ATPase activity of Sav1866 was more sensitive to sodium chloride and pH than the basal ATPase activity of Pgp. In the presence of the allocrite $C_{12}EO_8$, the pH sensitivity decreased considerably toward high pH values. A low pH sensitivity, especially toward high pH values, seems to correlate generally with a high catalytic efficiency and may be caused by a local pH decrease due to enhanced proton release upon ATP hydrolysis. A similar explanation may account for the lower sodium chloride sensitivity observed during vanadate inhibition experiments with Sav1866 in mixed lipid/$C_{12}E_8$ micelles.

Neutral allocrites seem to bind to the TMDs of the exporters at the level of the membrane−water interface via the formation of hydrogen bonds between H-bond acceptors in allocrites and H-bond donors in the exporter. The affinity of allocrites per hydrogen bond was lower for Sav1866 than for Pgp, which may explain the lack of binding of a second inhibitory molecule. In addition, Sav1866 showed a much stronger ability to flop hydrophobic amphiphiles as seen from a higher q ratio of >5 instead of a q of 2.7 for Pgp (where q is the ratio between the affinity of the detergent's anchor for the lipid membrane and the affinity of the detergent's headgroup for the exporter). Sav1866 thus resembles MsbA with respect to the higher concentration of half-maximal binding of ATP and with respect to its ability to handle more hydrophobic amphiphiles than Pgp.

AUTHOR INFORMATION

Corresponding Author

*Telephone: +41-61-267 22 06. Fax: +41-61-267 21 89. E-mail: anna.seelig@unibas.ch.

Present Addresses

[§]A.B.: Syngenta Crop Protection Münchwilen AG, Schaffhauserstrasse 101, CH-4332 Stein, Switzerland.

[∥]P.Ä.: Actelion Pharmaceuticals Ltd., Gewerbestrasse 16, 4123 Allschwil, Switzerland.

Author Contributions

A.B., P.Ä., and X.L.-B. contributed equally to this work.

Funding

This work was supported by Swiss National Science Foundation Grant 31003A-129701.

Notes

The authors declare no competing financial interest.

■ ABBREVIATIONS

ABC, ATP-binding cassette; CMC, critical micelle concentration; C_w, concentration of water; ΔG^0_{lw}, free energy of lipid−water partitioning; $\Delta G^0_{tw(1)}$, free energy of binding from water to the transporter (exporter); $\Delta G^0_{tl(1)}$, free energy of binding from the lipid membrane to the transporter (exporter); K_1, concentration of half-maximal activity; $K_{0.5}$, ATP or allocrite concentration at which the binding sites are 50% occupied; K_{lw}, lipid−water partition coefficient; K_{tw}, transporter−water (exporter−water) binding constant; K_{tl}, transporter−lipid (exporter−lipid) binding constant; NBD, nucleotide-binding domain; Pgp, MDR1, and ABCB1, P-glycoprotein; q, $\Delta G^0_{lw}/\Delta G^0_{tl(1)}$ free energy ratio that reflects the ratio between the affinity of the detergent's anchor for the lipid membrane and the affinity of the detergent's headgroup for the exporter; RT, product of the gas constant and the absolute temperature; TMD, transmembrane domain.

■ ADDITIONAL NOTES

[a]The turnover number corresponds to the maximal number of allocrites moved from the cytoplasmic to the periplasmic membrane leaflet per time and exporter ($k_{cat} = V_{max}/$[exporter]). The basal turnover number could reflect the number of endogenous allocrites (for Pgp and Sav1866, e.g., a lipid molecule with a protonated phosphatidylcholine headgroup)[30] per time and exporter.

[b]To a first approximation the concentration of half-maximal activation, K_1, the concentration of half-maximal binding $K_{0.5}$, and the dissociation constant K_d are comparable under the present conditions.

■ REFERENCES

(1) Zolnerciks, J. K., Andress, E. J., Nicolaou, M., and Linton, K. J. (2011) Structure of ABC transporters. *Essays Biochem. 50*, 43−61.

(2) Davidson, A. L., Dassa, E., Orelle, C., and Chen, J. (2008) Structure, function, and evolution of bacterial ATP-binding cassette systems. *Microbiol. Mol. Biol. Rev. 72*, 317−364.

(3) Gottesman, M. M., and Pastan, I. (1993) Biochemistry of multidrug resistance mediated by the multidrug transporter. *Annu. Rev. Biochem. 62*, 385−427.

(4) Dawson, R. J., and Locher, K. P. (2006) Structure of a bacterial multidrug ABC transporter. *Nature 443*, 180−185.

(5) Dawson, R. J., and Locher, K. P. (2007) Structure of the multidrug ABC transporter Sav1866 from *Staphylococcus aureus* in complex with AMP-PNP. *FEBS Lett. 581*, 935−938.

(6) Ward, A., Reyes, C. L., Yu, J., Roth, C. B., and Chang, G. (2007) Flexibility in the ABC transporter MsbA: Alternating access with a twist. *Proc. Natl. Acad. Sci. U.S.A. 104*, 19005−19010.

(7) Hohl, M., Briand, C., Grutter, M. G., and Seeger, M. A. (2012) Crystal structure of a heterodimeric ABC transporter in its inward-facing conformation. *Nat. Struct. Mol. Biol. 19*, 395−402.

(8) Aller, S. G., Yu, J., Ward, A., Weng, Y., Chittaboina, S., Zhuo, R., Harrell, P. M., Trinh, Y. T., Zhang, Q., Urbatsch, I. L., and Chang, G. (2009) Structure of P-glycoprotein reveals a molecular basis for poly-specific drug binding. *Science 323*, 1718−1722.

(9) Zolnerciks, J. K., Wooding, C., and Linton, K. J. (2007) Evidence for a Sav1866-like architecture for the human multidrug transporter P-glycoprotein. *FASEB J. 21*, 3937−3948.

(10) O'Mara, M. L., and Tieleman, D. P. (2007) P-glycoprotein models of the apo and ATP-bound states based on homology with Sav1866 and MalK. *FEBS Lett. 581*, 4217−4222.

(11) Jardetzky, O. (1966) Simple allosteric model for membrane pumps. *Nature 211*, 969−970.

(12) Seelig, A. (2007) The role of size and charge for blood-brain barrier permeation of drugs and fatty acids. *J. Mol. Neurosci. 33*, 32−41.

(13) Nervi, P., Li-Blatter, X., Aanismaa, P., and Seelig, A. (2010) P-glycoprotein substrate transport assessed by comparing cellular and vesicular ATPase activity. *Biochim. Biophys. Acta 1798*, 515−525.

(14) Velamakanni, S., Yao, Y., Gutmann, D. A., and van Veen, H. W. (2008) Multidrug transport by the ABC transporter Sav1866 from *Staphylococcus aureus*. *Biochemistry 47*, 9300−9308.

(15) Li-Blatter, X., Nervi, P., and Seelig, A. (2009) Detergents as intrinsic P-glycoprotein substrates and inhibitors. *Biochim. Biophys. Acta 1788*, 2335−2344.

(16) Li-Blatter, X., and Seelig, A. (2010) Exploring the P-glycoprotein binding cavity with polyoxyethylene alkyl ethers. *Biophys. J. 99*, 3589−3598.

(17) Li-Blatter, X., Beck, A., and Seelig, A. (2012) P-Glycoprotein-ATPase Modulation: The Molecular Mechanisms. *Biophys. J. 102*, 1383−1393.

(18) Litman, T., Zeuthen, T., Skovsgaard, T., and Stein, W. D. (1997) Structure-activity relationships of P-glycoprotein interacting drugs: Kinetic characterization of their effects on ATPase activity. *Biochim. Biophys. Acta 1361*, 159−168.

(19) Gatlik-Landwojtowicz, E., Aanismaa, P., and Seelig, A. (2006) Quantification and characterization of P-glycoprotein-substrate interactions. *Biochemistry 45*, 3020−3032.

(20) Orlowski, S., Selosse, M. A., Boudon, C., Micoud, C., Mir, L. M., Belehradek, J., Jr., and Garrigos, M. (1998) Effects of detergents on P-glycoprotein atpase activity: Differences in perturbations of basal and verapamil-dependent activities. *Cancer Biochem. Biophys. 16*, 85−110.

(21) Doige, C. A., Yu, X., and Sharom, F. J. (1993) The effects of lipids and detergents on ATPase-active P-glycoprotein. *Biochim. Biophys. Acta 1146*, 65−72.

(22) Urbatsch, I. L., Sankaran, B., Bhagat, S., and Senior, A. E. (1995) Both P-glycoprotein nucleotide-binding sites are catalytically active. *J. Biol. Chem. 270*, 26956−26961.

(23) Borths, E. L., Poolman, B., Hvorup, R. N., Locher, K. P., and Rees, D. C. (2005) In vitro functional characterization of BtuCD-F, the *Escherichia coli* ABC transporter for vitamin B12 uptake. *Biochemistry 44*, 16301−16309.

(24) Itaya, K., and Ui, M. (1966) A new micromethod for the colorimetric determination of inorganic phosphate. *Clin. Chim. Acta 14*, 361−366.

(25) Edelhoch, H. (1967) Spectroscopic determination of tryptophan and tyrosine in proteins. *Biochemistry 6*, 1948−1954.

(26) Walker, J. M. (2005) pp 571−607, Humana Press, Totowa, NJ.

(27) Aanismaa, P., and Seelig, A. (2007) P-Glycoprotein Kinetics Measured in Plasma Membrane Vesicles and Living Cells. *Biochemistry 46*, 3394−3404.

(28) Gordon, J. A. (1991) Use of vanadate as protein-phosphotyrosine phosphatase inhibitor. *Methods Enzymol. 201*, 477−482.

(29) Gatlik-Landwojtowicz, E., Aanismaa, P., and Seelig, A. (2004) The rate of P-glycoprotein activation depends on the metabolic state of the cell. *Biochemistry 43*, 14840−14851.

(30) Landwojtowicz, E., Nervi, P., and Seelig, A. (2002) Real-time monitoring of P-glycoprotein activation in living cells. *Biochemistry 41*, 8050−8057.

(31) Beck, A., Li-Blatter, X., Seelig, A., and Seelig, J. (2010) On the interaction of ionic detergents with lipid membranes. Thermodynamic comparison of n-alkyl-+N(CH) and n-alkyl-SO. *J. Phys. Chem. B 114*, 15862−15871.

(32) Yang, J. T., Wu, C. S. C., and Martinez, H. M. (1986) Calculation of Protein Conformation from Circular Dichroism. *Methods Enzymol. 130*, 208−269.

(33) Boguslavsky, V., Rebecchi, M., Morris, A. J., Jhon, D. Y., Rhee, S. G., and McLaughlin, S. (1994) Effect of monolayer surface pressure on the activities of phosphoinositide-specific phospholipase C-β1, -γ1, and -δ1. *Biochemistry 33*, 3032−3037.

(34) Fischer, H., Gottschlich, R., and Seelig, A. (1998) Blood-brain barrier permeation: Molecular parameters governing passive diffusion. *J. Membr. Biol. 165*, 201−211.

(35) Seelig, A. (1987) Local anesthetics and pressure: A comparison of dibucaine binding to lipid monolayers and bilayers. *Biochim. Biophys. Acta 899*, 196−204.
(36) Sharom, F. J., Yu, X., Chu, J. W., and Doige, C. A. (1995) Characterization of the ATPase activity of P-glycoprotein from multidrug-resistant Chinese hamster ovary cells. *Biochem. J. 308* (Part 2), 381−390.
(37) Zaitseva, J., Jenewein, S., Wiedenmann, A., Benabdelhak, H., Holland, I. B., and Schmitt, L. (2005) Functional characterization and ATP-induced dimerization of the isolated ABC-domain of the haemolysin B transporter. *Biochemistry 44*, 9680−9690.
(38) Hoffman, A. D., Urbatsch, I. L., and Vogel, P. D. (2010) Nucleotide binding to the human multidrug resistance protein 3, MRP3. *Protein J. 29*, 373−379.
(39) Kerr, K. M., Sauna, Z. E., and Ambudkar, S. V. (2001) Correlation between steady-state ATP hydrolysis and vanadate-induced ADP trapping in Human P-glycoprotein. Evidence for ADP release as the rate-limiting step in the catalytic cycle and its modulation by substrates. *J. Biol. Chem. 276*, 8657−8664.
(40) Al-Shawi, M. K., and Senior, A. E. (1993) Characterization of the adenosine triphosphatase activity of Chinese hamster P-glycoprotein. *J. Biol. Chem. 268*, 4197−4206.
(41) Sharom, F. J., Yu, X., and Doige, C. A. (1993) Functional reconstitution of drug transport and ATPase activity in proteoliposomes containing partially purified P-glycoprotein. *J. Biol. Chem. 268*, 24197−24202.
(42) Schwyzer, R. (1987) Membrane-assisted molecular mechanism of neurokinin receptor subtype selection. *EMBO J. 6*, 2255−2259.
(43) Seitz, H. R., Heck, M., Hofmann, K. P., Alt, T., Pellaud, J., and Seelig, A. (1999) Molecular determinants of the reversible membrane anchorage of the G-protein transducin. *Biochemistry 38*, 7950−7960.
(44) Heerklotz, H., and Seelig, J. (2000) Correlation of membrane/water partition coefficients of detergents with the critical micelle concentration. *Biophys. J. 78*, 2435−2440.
(45) Heerklotz, H., and Seelig, J. (2000) Titration calorimetry of surfactant-membrane partitioning and membrane solubilization. *Biochim. Biophys. Acta 1508*, 69−85.
(46) Meier, M., Blatter, X. L., Seelig, A., and Seelig, J. (2006) Interaction of verapamil with lipid membranes and P-glycoprotein: Connecting thermodynamics and membrane structure with functional activity. *Biophys. J. 91*, 2943−2955.
(47) Kamaraju, K., and Sukharev, S. (2008) The membrane lateral pressure-perturbing capacity of parabens and their effects on the mechanosensitive channel directly correlate with hydrophobicity. *Biochemistry 47*, 10540−10550.
(48) McLaughlin, S. (1977) Electrostatic potentials at membrane-solution interfaces. *Curr. Top. Membr. Transp.*, 71−144.
(49) Eckford, P. D., and Sharom, F. J. (2008) Functional characterization of *Escherichia coli* MsbA: Interaction with nucleotides and substrates. *J. Biol. Chem. 283*, 12840−12850.
(50) Aanismaa, P., Gatlik-Landwojtowicz, E., and Seelig, A. (2008) P-glycoprotein senses its substrates and the lateral membrane packing density: Consequences for the catalytic cycle. *Biochemistry 47*, 10197−10207.
(51) Nebel, S., Ganz, P., and Seelig, J. (1997) Heat changes in lipid membranes under sudden osmotic stress. *Biochemistry 36*, 2853−2859.
(52) Benabdelhak, H., Schmitt, L., Horn, C., Jumel, K., Blight, M. A., and Holland, I. B. (2005) Positive co-operative activity and dimerization of the isolated ABC ATPase domain of HlyB from *Escherichia coli*. *Biochem. J. 386*, 489−495.
(53) Delannoy, S., Urbatsch, I. L., Tombline, G., Senior, A. E., and Vogel, P. D. (2005) Nucleotide binding to the multidrug resistance P-glycoprotein as studied by ESR spectroscopy. *Biochemistry 44*, 14010−14019.
(54) Ernst, R., Koch, J., Horn, C., Tampe, R., and Schmitt, L. (2006) Engineering ATPase activity in the isolated ABC cassette of human TAP1. *J. Biol. Chem. 281*, 27471−27480.
(55) Al-Shawi, M. K., Polar, M. K., Omote, H., and Figler, R. A. (2003) Transition state analysis of the coupling of drug transport to ATP hydrolysis by P-glycoprotein. *J. Biol. Chem. 278*, 52629−52640.